Advanced Fiber Materials
https://doi.org/10.1007/s42765-021-00105-8

RESEARCH ARTICLE

Electrospinning of Neat Graphene Nanofibers

Zhanpo Han[1,3] · Jiaqing Wang[1] · Senping Liu[1] · Qinghua Zhang[2] · Yingjun Liu[1] · Yeqiang Tan[2,3] · Shiyu Luo[1] · Fan Guo[1] · Jingyu Ma[1] · Peng Li[1] · Xin Ming[1] · Chao Gao[1] · Zhen Xu[1]

Received: 25 June 2021 / Accepted: 11 September 2021

Abstract

Macroscopic assembly of graphene sheets has renovated the preparation of neat carbonaceous fibers with integrating high performance and superior functionalities, beyond the pyrolysis of conventional polymeric precursors. To date, graphene microfibers by the liquid crystalline wet-spinning method have been established. However, how to reliably prepare continuous neat graphene nanofibers remains unknown. Here, we present the electrospinning of neat graphene nanofibers enabled by modulating colossally extensional flow state of graphene oxide liquid crystals. We use polymer with mega molecular weight as transient additives to realize the colossal extensional flow and electrospinning. The neat graphene nanofibers feature high electronic quality and crystallinity and exhibit high electrical conductivity of 2.02×10^6 S/m that is to be comparable with single crystal graphite whisker. The electrospinning of graphene nanofibers was extended to prepare large-area fabric with high flexibility and superior specific electrical/thermal conductivities. The electrospinning of graphene nanofibers opens the door to nanofibers of rich two-dimensional sheets and the neat graphene nanofibers may grow to be a new species after conventional carbonaceous nanofibers and whiskers in broad functional applications.

Keywords Electrospinning · Graphene nanofiber · Functional fabrics

Introduction

Continuous carbonaceous fibers are conventionally fabricated by the long prevailing pyrolysis of precursor fibers of polymers or small molecules, such as the prevailing PAN and pitch, extending from microfibers to nanofibers [1–6]. The emerged processible graphene has initiated a new paradigm to fabricate carbonaceous fibers by the ordered assembly of graphene derivatives, notably exemplified by graphene oxide (GO) [7–10]. In the past decade, graphene microfibers have been wet-spun from GO liquid crystals and this new fiber with the radial size of 5–100 μm has exhibited superior functionalities to conventional PAN- and pitch-based carbon fibers, accompanying with the ever-growing mechanical strength [9, 11–14]. For example, the record thermal conductivity (1480 W/mK) of crystalline graphene fiber is much higher than that of meso-pitch based carbon fiber (1000 W/mK) [15]. These merits of graphene microfibers justify the superiority of macroscopic assembly philosophy for the future disruptive carbonaceous fibers. Considerable advances in graphene microfibers intuitively encourage us to extend the superiority of bottom-up assembly of graphene to nanofibers with expected superior functionalities.

✉ Yingjun Liu
yingjunliu@zju.edu.cn

✉ Yeqiang Tan
tanyeqiang@qdu.edu.cn

✉ Chao Gao
chaogao@zju.edu.cn

✉ Zhen Xu
zhenxu@zju.edu.cn

[1] MOE Key Laboratory of Macromolecular Synthesis and Functionalization, Department of Polymer Science and Engineering, Key Laboratory of Adsorption and Separation Materials and Technologies of Zhejiang Province, Zhejiang University, 38 Zheda Road, Hangzhou 310027, People's Republic of China

[2] State Key Laboratory for Modification of Chemical Fibers and Polymer Materials, Donghua University, Shanghai 200051, People's Republic of China

[3] State Key Laboratory of Bio-Fibers and Eco-Textiles, Collaborative Innovation Center of Marine Biobased Fiber and Ecological Textile Technology, School of Materials Science and Engineering, Qingdao University, Qingdao 266071, People's Republic of China

Published online: 16 November 2021

Assembling two-dimensional GO sheets into 1D nano fibrous form is a topology transformation process, which has been tried by several methods [7, 16–18]. Freeze-drying and templated wrapping have been proposed to prepare graphene nanoscrolls and nanotubes, but with short length far below 1 mm. Solution deposition of GO through a miniature nozzle has tried to print nanofibers, but at an extremely slow speed of 140 μm/s [19]. As an advanced nanofiber spinning method, electrospinning technology is rapidly developing into coaxial, side-by-side, triaxial and other complex multi-fluid processes and has produced rich fibrous materials with advanced functionalized structures [20, 21]. The range of electrospun fibers has been limited in the polymeric range with considerable stretchability of spinning dope. For the new 2D sheets, electrospinning can produce their polymer-based composite nanofibers with less than 5% graphene content [22]. The production of composite nanofibers with high graphene content by electrospinning is still an urgent problem to be solved [23]. On the one hand, the excessive polymer matrix degrades functionalities and even generates discontinuous fibers or powders after thermal annealing. On the other hand, the increasing of GO content greatly depresses the viscoelasticity of polymer and thus disables the electrospinning [24]. To date, the reliable preparation of neat continuous graphene nanofibers (GNFs) has not yet been achieved. How to continuously proceed the topology transformation to get neat GNF remains a great challenge.

Here, we realize the electrospinning of neat GNFs by achieving the colossal extension flow state of GO-rich dispersions. We choose polymer with mega molecular weight as the small-fraction transient additive to enable the colossal extension of GO dispersions and stable electrospinning. The minimum content of polymer (<35%) ensures the continuous length up to decimeters, high electronic quality and crystallinity of neat GNFs with the diameter of 100–900 nm. The electrospun GNFs exhibit high electrical conductivity of 2.02×10^6 S/m, approaching that of single-crystal graphite [25]. The confinement in the highly extensional thread guides the continuous topology transformation and GNFs feature compact scrolling structure. We also fabricate large-area GNF fabrics with good flexibility, high strength, and superior electrical/thermal conductivities. The neat GNF may emerge as a new species beyond conventional carbonaceous nanofibers and graphite whiskers, with promising values for applications of advanced composites, electrodes, catalysts, sensors and thermal managements [16, 26].

Experimental Section

Materials

Aqueous GO dispersions (average lateral size of 30 μm) were purchased from Hangzhou Gaoxi Technology Co. Ltd (www.gaoxitech.com). Other reagents were purchased from Sinopharm Chemical Reagent Co., Ltd and used as received.

Preparation of Spinning Dope

The GO dispersion (20 mg/mL), the PAS solution (20 mg/mL) and Triton X-100, were evenly mixed in different proportions. Followed by removing possible impurities and degassing treatment, GO/PAS dopes were obtained.

Fabrication of GNFs via Electrospinning

Briefly, GO/PAS dopes were successively pumped at a flow rate of 0.15 mL/min using a syringe pump and electrospun under a potential of 15–30 kV between the spinneret (30 Gauge needle) and a grounded bronze base collector. The temperature and the humidity in the chamber of the electrospinning setup were kept at 60 ℃ and 10%, respectively. Parallel collecting plates were used to collect the graphene nanofiber network. A high-speed drum was used to collect fabrics with orientated structure. The precursor GO/PAS nanofibers were reduced by hydroiodic acid (HI) at 90 ℃ for 12 h to get rGNFs and heating to 3000 ℃ at a rate of 10 ℃ min^{-1} in a flow of argon to get final neat GNF.

Calculation of Layer Number and Sheet Diameter of Graphene in Fiber

For the nanofibers composed of few layers GO platelets, the number of GO (N) occupying the fiber section can be estimated from the cross-sectional area under a certain GO percentage (ω).

$$N(L \bullet d) = A \bullet \omega$$

where L is the average size of GO, d is the interlayer spacing, A is the cross-sectional area of a nanofiber that is equal to $\pi < R/2 >^2$.

Characterization

The fiber morphology was characterized by a field-emission scanning electron microscope (Hitachi, S4800). The atomic-scale microstructures of the nanofibers were further characterized by a transmission electron microscope (JEM, 2100F). Raman spectra were collected on a Renishaw in Via-Reflex Raman microscope with a 532 nm laser source. The rheological properties of dopes were measured on an Anton Paar MCR 302. The surface tension of dopes was measured on a Dataphysics OCA20. An empirical formula was used to calculate the coherence crystalline domain by the integrated intensity ratio of D band and G band [44]. X-ray diffraction

measurements were taken on a Philips X'Pert PRO diffractometer using Cu Kα1 radiation (40 kV, 40 mA) with an X-ray wavelength (λ) of 1.5418 Å. XPS was performed using a PHI 5000C ESCA system operated at 14.0 kV. All binding energies were referenced to the C1s neutral carbon peak at 284.8 eV. Tensile strength testing was conducted using a Keysight T150 UTM and Instron 2344. The gauge length in tensile tests is 10 mm. The electrical conductivity was measured by a standard four-probe method. Thermal conductivity was measured utilizing a well-established self-heating method in a vacuum. At least three measurements were carried out for the average value of electrical and thermal conductivities.

Results and Discussion

Electrospinning is an efficient approach to fabricate nanofibers by colossally stretching the spinning dopes under high accelerating electric field [27, 28]. Neat GO liquid crystalline dispersions have poor stretchability for the lack of chain entanglement as usual polymers, that denies the possibility of electrospinning (Fig. 1a). To enable the electrospinning of GO, we introduced polyacrylate sodium (PAS) with extremely high molecular weight ($\sim 1 \times 10^8$ g/mol) and an accessory surfactant of Triton X-100 into GO dispersions [29–32]. The addition of PAS and Triton X-100 adjusted the rheological properties and surface tension of GO dopes (Fig. S1). Uniaxial extension tests demonstrated that the stretchability of GO/PAS monotonically increases with increasing PAS content (Fig. 1b and Fig. S2). The extension ratio shows one order of magnitude enhancement from 40% of neat GO dispersions to 340% of the GO/PAS dopes with a PAS content of 80%. Even a low content of 20% causes a 3.7 times larger extension ratio than that of neat GO dispersions. The mega PAS effectively counteracts the intrinsic barrier effect of 2D GO, that disrupts the continuity of polymer entanglement network, thus endows GO/PAS dopes with colossal stretchability [33, 34].

For GO aqueous dispersions with PAS content higher than 20%, we proceeded the electrospinning on a simple apparatus at the surrounding temperature of 60 °C to prevent the collapse of fibers by moisture adsorption (Video S1, Supporting Information). Continuous threads were stretched out from the nozzle (positive electrode) and fled to deposit onto collectors (negative electrode) under high electric field of 15–30 kV/cm (Fig. 1c and Fig. S3). The collected fibers formed interconnected networks and the thickness of intertwined membranes was controlled by the collecting time, evolving from a transparent film at 10 min to a semi-transparent film at 30 min (Fig. 1d). Due to the colossal stretching under electric acceleration, the diameter of jet threads was considerably thinned down to 7 μm, and the collected fibers have diameters of hundreds of nanometers after drying. Figure 1e shows the typical morphology of GO/PAS nanofibers with a diameter of ~ 500 nm, which is much thinner than that of reported wet-spun GO fibers [11]. The precursor GO/PAS nanofibers were chemically reduced (denotes as rGNF) and thermally annealed at high temperature up to 3000 °C to get neat GNFs (GNF-3000) to remove polymer additives. Hereafter, the term GNFs refers to samples annealed at 3000 °C unless otherwise stated. For the first time, we used the electrospinning method to proceed the topology transition from planar GO to 1D nanofibers and obtained continuous neat GNFs.

The morphology of the electrospun nanofibers strongly depends on the viscoelasticity of spinning dope, jet speed, drying velocity and surface tension [27, 35–39]. In the collection of GO/PAS nanofibers, we observed three typical morphologies: beads, bead-on-string and continuous fibers (Fig. 2a, b). In principle, the liquid threads either can be pinched off by the surface tension to form drops or intermediate bead-on-string structures for the Raleigh instability, or directly dried to nanofibers before pinching off. We concluded a morphology diagram correlated with the PAS content and GO concentration (Fig. 2c). For the neat GO/PAS dope, beads and bead-on-string morphologies dominated. We further introduced Triton surfactant to weaken the pinching off trend by lowering the surface tension (Figure S1) and obtained homogeneous nanofibers in the GO concentration range higher than 7 mg/cm^3. The minimum content of Triton to ensure the fiber morphology decreases as GO concentration increases, which brings an improved rigidity of liquid threads to resist the pinching-off trend. The collection efficiency of nanofibers increased with Triton, reaching 78% at a content of 20% (Fig. 2d).

In the optimized composition range for bead-free fibers, we controlled the fiber diameter by adjusting the solid content of spinning dope and the corresponding GO concentration (Fig. 2e–h, Fig. S4). The diameter of electrospun fibers has a broad distribution, which is possibly caused by wide size distribution of GO sheets (~ 8–45 μm) and the non-uniform stretching [40, 41]. At the extreme available voltage, the average diameter (< R >) decreased from 615 to 195 nm when GO concentration decreased from 10 mg/g to 6 mg/g. Actually, we attained the size limit of 1D assembly of GO. Guided by the mass conservation principle, it can be deduced that the nanofiber with < R > of 195 nm is wrapped by several (1–5) GO sheets with lateral size of 8–45 μm (the calculation details see experimental section).

Given that the average lateral size (~ 30 μm) of GO sheets is nearly two orders of magnitude larger than the diameter (195–615 nm) of electrospun GNFs, it is undoubtedly deduced that GO sheets continuously rolled to form

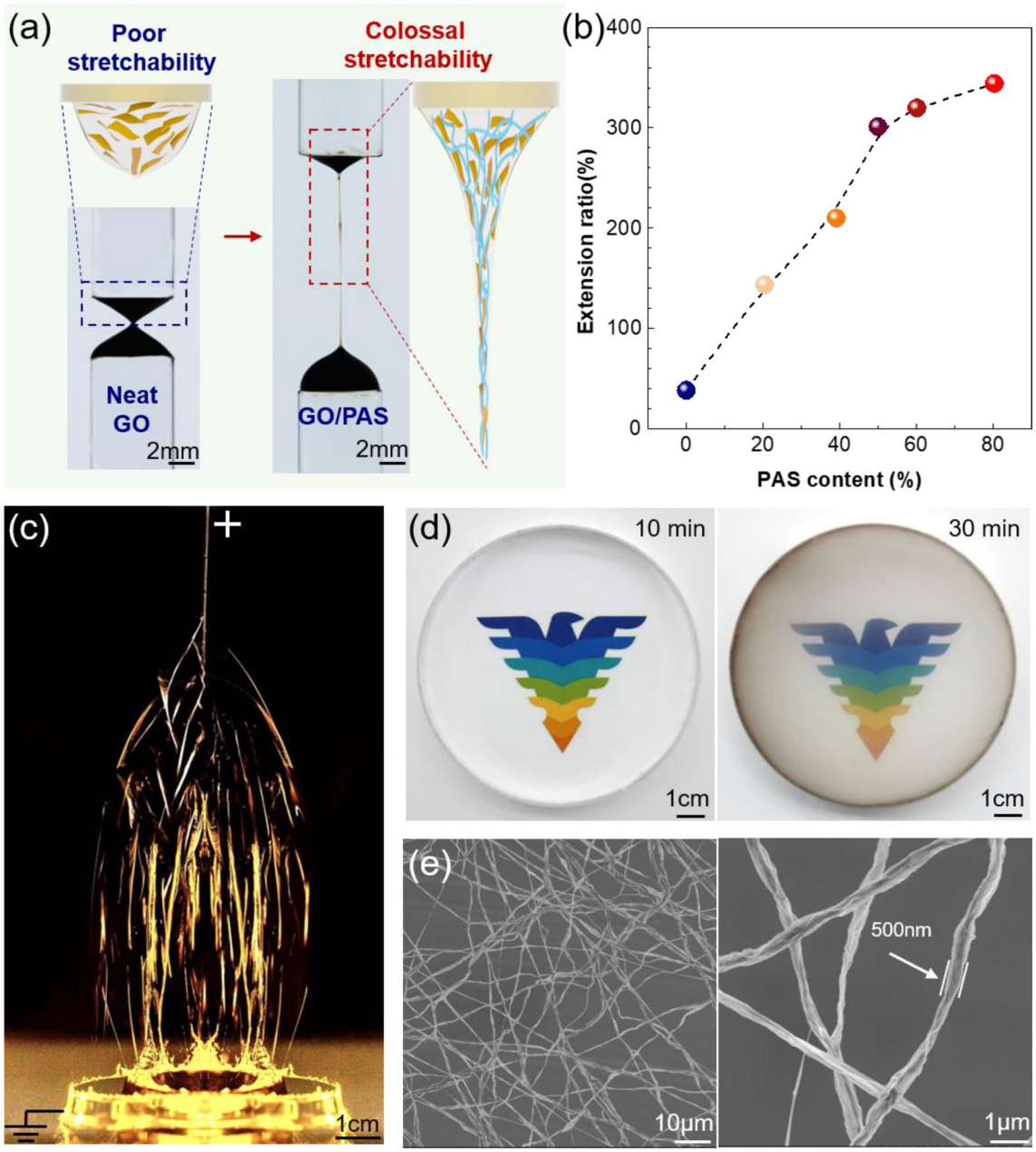

Fig. 1 The electrospinning of GO nanofibers. **a** The comparison of extension states and constituent illustrations of pure GO and GO/PAS spinning dopes. **b** The extension ratio of GO/PAS dope as a function of PAS containing. **c** Photograph of continuous jet threads stretching out from the nozzle. **d** GO/PAS nanofiber membranes at different collecting time. **e** SEM images of electrospun GO/PAS nanofibers

nanofibers. The continuous length of collected GNFs is dozens of centimeters (Fig. 3a), four orders of magnitude longer than the average size of GO, suggesting that GO sheets should interconnect with each other to become continuous. In comparison, the radial size of GNFs is only one fiftieth of the usual diameter of wet-spun graphene fibers (Fig. 3b). We tested the mechanical strength of rGNF and found that the thinning of fiber diameter induces an increasing of tensile strength (Fig. 3c and Fig. S6), from the 2.5 GPa of wet-spun reduced GF (< R > of ~ 7 μm) [11] to 4.3 GPa of our rGNF (< R > of 0.8 μm), exhibiting a Hall Patch effect with an index of -0.3. The increasing trend of strength with decreasing radial size is possibly caused by the more compact structure in rGNF with fewer defects [13].

By structural analyses by SEM and TEM, we concluded the structural mode of GNF to include three major

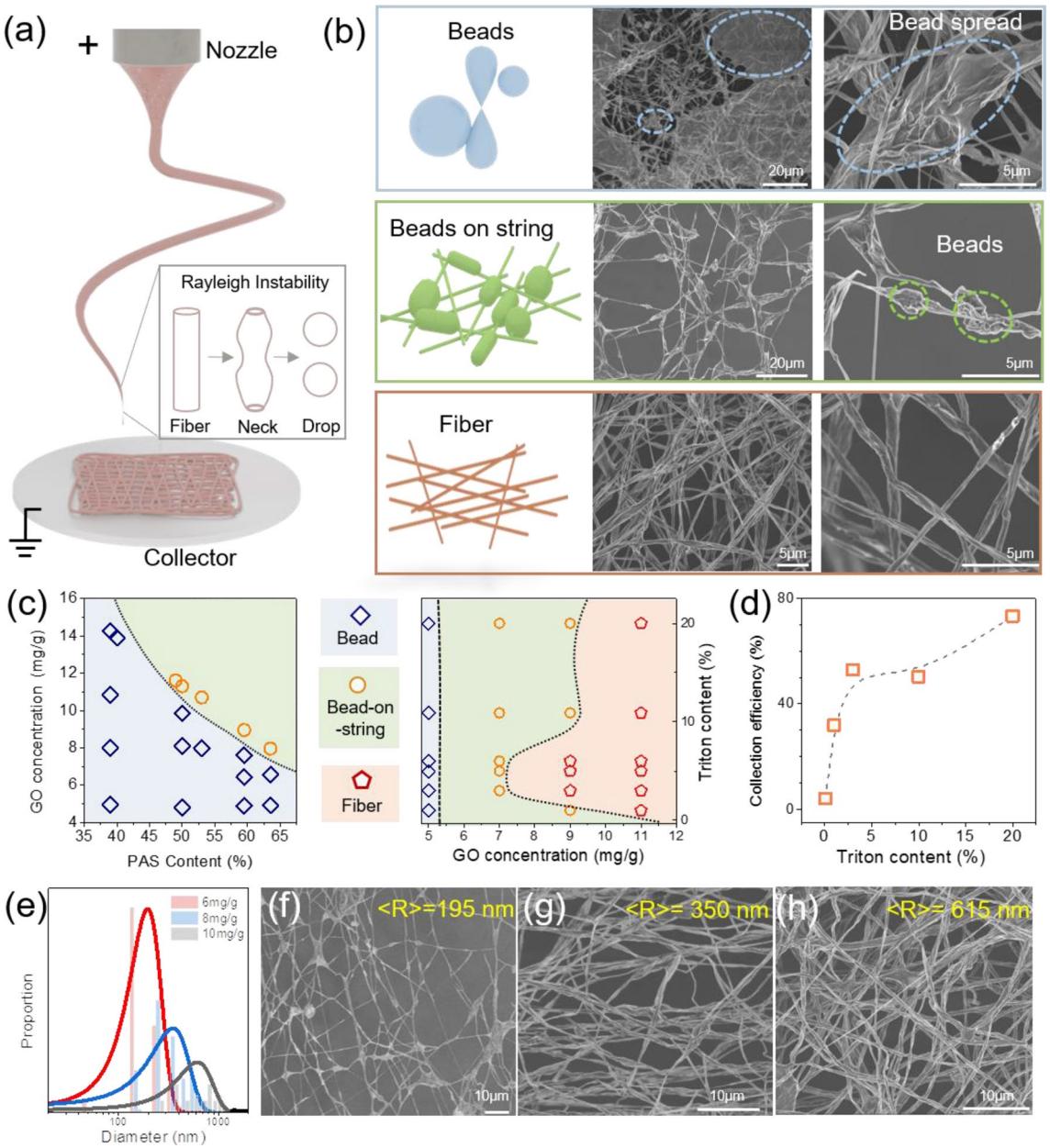

Fig. 2 The morphology and diameter control of GO/PAS nanofibers. **a** The formation mechanism of nanofibers and beads of electrospinning. **b** Three morphology modes of GO/PAS nanofibers: beads, beads-on-string and fiber. **c** Morphology diagram correlated with the PAS content and GO concentration. **d** The collection efficiency of nanofibers with Triton content. Statistic chart of the average diameters (**e**) and SEM images (**f**–**h**) of nanofibers with increasing GO concentrations

characteristics: aligned folds, interlayer overlapping and multilayer rolling (Fig. 3d). The surface of GNFs features aligned folds along the fiber axis resulting from the radial shrinkage of highly stretched electrospun threads after drying. The surface folds have a typical length of ~ 200 nm and a width of 20–60 nm (Fig. 3f), which are much smaller than those (length of 20 μm and width of 200–600 nm) of wet-spun graphene fibers (Fig. 3b) [7]. Cross-section morphology reveals that graphene sheets are overlapped to form continuous fibers and these multilayers are rolled together to form a scrolled laminated structure with ridges and kinks (Fig. 3h). Distinct from the various disclination strength of wrinkles in wet-spun microfibers, the wrinkles of graphene laminates on the section of GNFs uniformly show a disclination strength (m) of 1/2, which can be seemed as the basic crystalline domain of microfibers (Fig. 3e) [11].

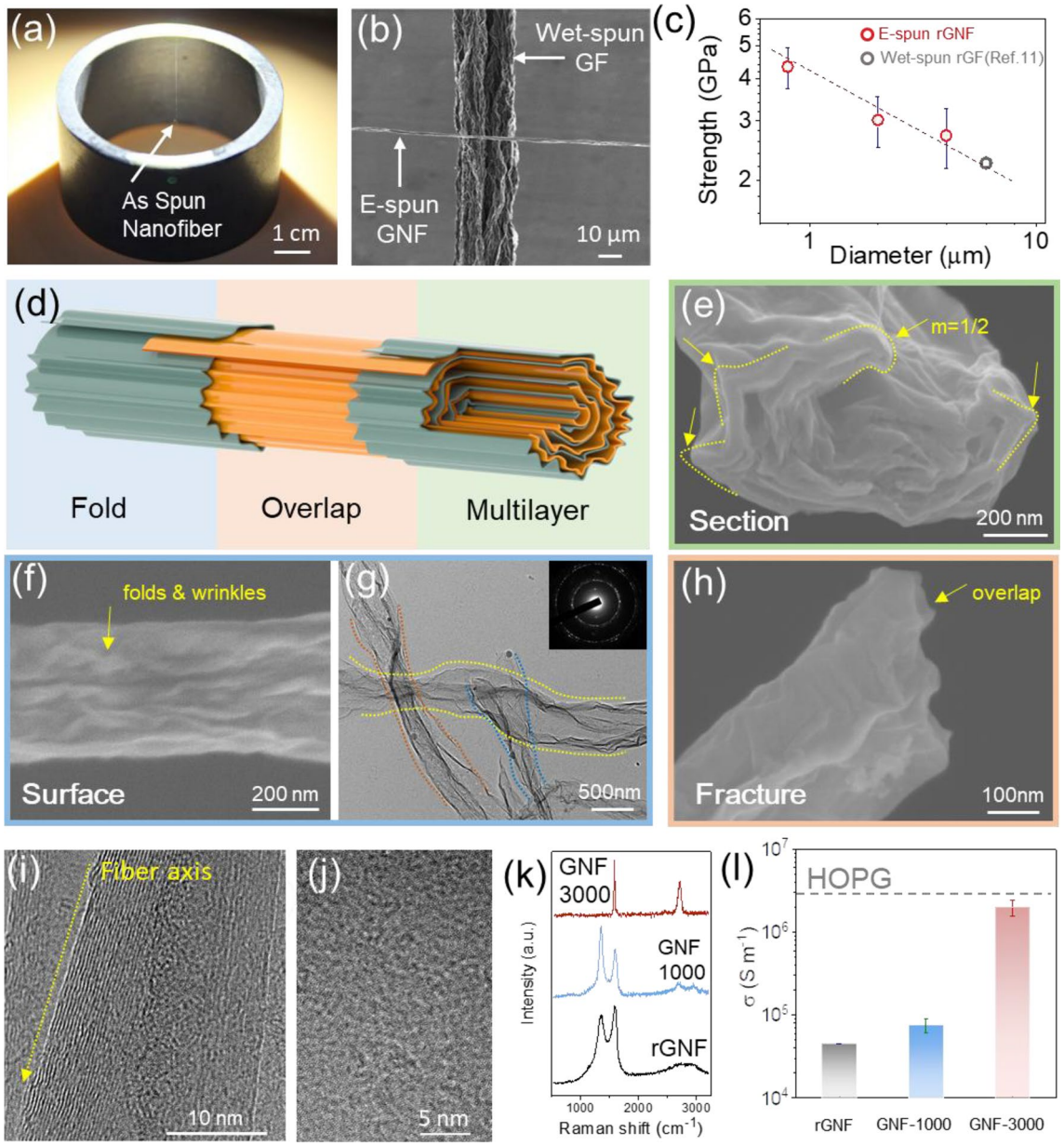

Fig. 3 Structural analysis of electrospun GNF. **a** Photograph of single continuous GO/PAS nanofiber. **b** The comparison of diameter of the wet-spun graphene microfiber and electrospun graphene nanofiber under SEM. **c** The mechanical strength of rGNF as a function of fiber diameter. **d** Schematic structure of GNFs. Microscopy images of the section (**e**), surface (**f**, **g**) and side facture (**h**) of GNFs. **i** and **j** TEM images of GNFs thermally annealed at 3000 ℃. Raman spectra (**k**) and electrical conductivity (**l**) of nanofibers annealed at different temperatures

We estimated that GNFs with a diameter of 400 nm consisted of 4–23 rolled graphene sheets, approaching the limit size of assembled graphene fibers.

In the thermal annealing process, the PAS was completely removed and nanofibers kept structural continuity and crystalline integrity, as in the case of wet-spun graphene fibers [11]. The sharp diffraction spots in SEAD pattern (insert in Fig. 3g) denote the high crystallinity of constituent graphene sheets in GNF [42, 43]. Closer inspections demonstrate that the large domain size (> 50 nm at least) of laminate graphene sheets with an interlayer spacing of 0.33 nm, close to the (002) lattice parameter (0.335) of single crystalline graphite (Fig. 3i). The planar domain in GNFs exhibits a complex Moiré pattern (Fig. 3j), indicating the randomly

twisted configuration of rolled graphene sheets, in accordance with multi discrete spots in Fig. 3g. Raman spectrum of the final GNFs (GNF-3000) shows a neglectable D peak, suggesting an effective recovery of structural defects due to the complete removal of oxygen-containing groups of GO sheets (Fig. 3k). The crystallite size in GNF-3000 was calculated as 640 nm from the integrated intensity ratio of D-band and G-band, which is orders of magnitude larger than the nanocrystalline graphitic domains inside the PAN-based carbon nanofibers, approaching the high crystalline quality of graphite whiskers [11, 44–46]. The merit of high crystallinity of GNFs possibly originates from the 2D precursor of GO that facilitates the growth of larger graphitic crystalline domain.

The high crystallinity (Fig. 3i–k and Fig. S5) awards GNFs high electrical conductivity (σ) that is comparable to highly oriented pyrolytic graphite (HOPG). As the thermal annealing temperature raised, the σ of nanofiber increased from 3×10^4 S/m of rGNF to 2.02×10^6 S/m of GNF-3000. The achieved high σ outperforms the benchmark PAN-based carbon nanofiber (3.8×10^5 S/m) [47], even approaching that (2.2×10^6 S/m) of HOPG (Fig. 3l). Importantly, the high σ extends to a length scale of several centimeters, which means the continuous crystalline domain along the axial direction of GNF. Considering the high σ and its length continuity, GNFs emerge as a new carbonaceous nanofiber species to be on a par with the vapor grown whiskers [48–50], but can be prepared by a continuous electrospinning method with high efficiency and directly processed into carbon fabrics.

The electrospun GNFs can be continuously shaped into fabrics with high flexibility and high electrical/thermal conductivities. By controlling the collection manner, GNF fabrics (GFFs) can be made to have random and aligned texture (Fig. 4 and Fig. S7). As shown in Fig. 4a–c, direct collection onto metal meshes obtained fabrics with random distribution of GNFs and thick fabrics can be peeled off to become a large-area free-standing film (such as 64 cm^2 in Fig. 4b). GNF fabric is lightweight, for example, it has the packing density of 350 mg/cm^3 and corresponding porosity of 76.1%. The GFF exhibited high flexibility and can be folded into a complicated origami with complex deformations and unfolded to initial flat state without any breakage, because that the ultrafine GNFs network can endure bending and even folding (Fig. 4c). The crystalline integrity of single GNF endows random GFFs (density of 0.22 g/cm^3) with high electrical conductivity (1.8×10^4 S/m) and thermal conductivity (62 W/mK in Fig. 4d, and Fig. S8), which are higher than those of PAN-based nanofiber fabrics (1.7×10^4 S/m and 20 W/mK) at the same density [51]. Moreover, GFFs exhibited a superiority in specific thermal and electrical conductivities to outperform prevailing carbon papers and fibrous films, including multiwalled carbon nanotube films, chemical reduced graphene films and thermally annealed graphene films (Fig. 4e) [15, 52–55]. Especially, the specific thermal conductivity of GFFs is close to the vaule of HOPG, exhibiting great potentials as nanofillers for thermally conductive composites [24].

We further used a high-speed drum to guide the alignment of electrospun nanofibers (Fig. 4f, g, and Fig. S9). The GNFs are well-aligned along the rotation direction (Fig. 4h, i) with an orientation order of 0.794 calculated by azimuthal scan curve of SAXS pattern (Figure S10) [56, 57]. The orientation brought 260% and 183% enhancements in strength and breakage elongation, respectively, as compared with the random GFFs (Fig. 4**j**). The alignment of GNFs brings high anisotropy in mechanical strength, strain, electrical and thermal conductivities (Fig. 4k). For example, the electrical conductivity in the orientation direction is 2.03×10^4 S/m, which is 1050% higher than that in the perpendicular direction of orientation, showing an anisotropic ratio of 11.5. Additionally, the high orientation improved the thermal conductivity of GFFs to 95 W/mK, much higher than that (62 W/mK) of random GFF and that (20 W/mK) of PAN-based nanofiber fabrics [58, 59]. The orientation of GNFs in fabrics offers a protocol to design and fabrication of networks to harness the favorable properties of GNFs for advanced composites [60–64].

Conclusion

In conclusion, we realized the electrospinning of neat graphene nanofibers by enabling the colossally extensional flow of GO liquid crystals with the assistance of mega polymer. The created colossally extensional flow state of 2D sheets extends the processing capability for fabricating as-design structures. The prototype electrospinning of graphene nanofibers can be developed as a general method to direct to new multifunctional nanofibers of board members of 2D sheets family, such as MXene, MoS_2 and so on. The prepared graphene nanofibers approach the size limit of 1D topology transformation and its conductivity is close to the bench mark single crystal whiskers. The continuously spun graphene nanofiber emerges as a useful nanofiber species with combining high performances and superior functionalities for many applications in energy storage, advanced composites and sensors.

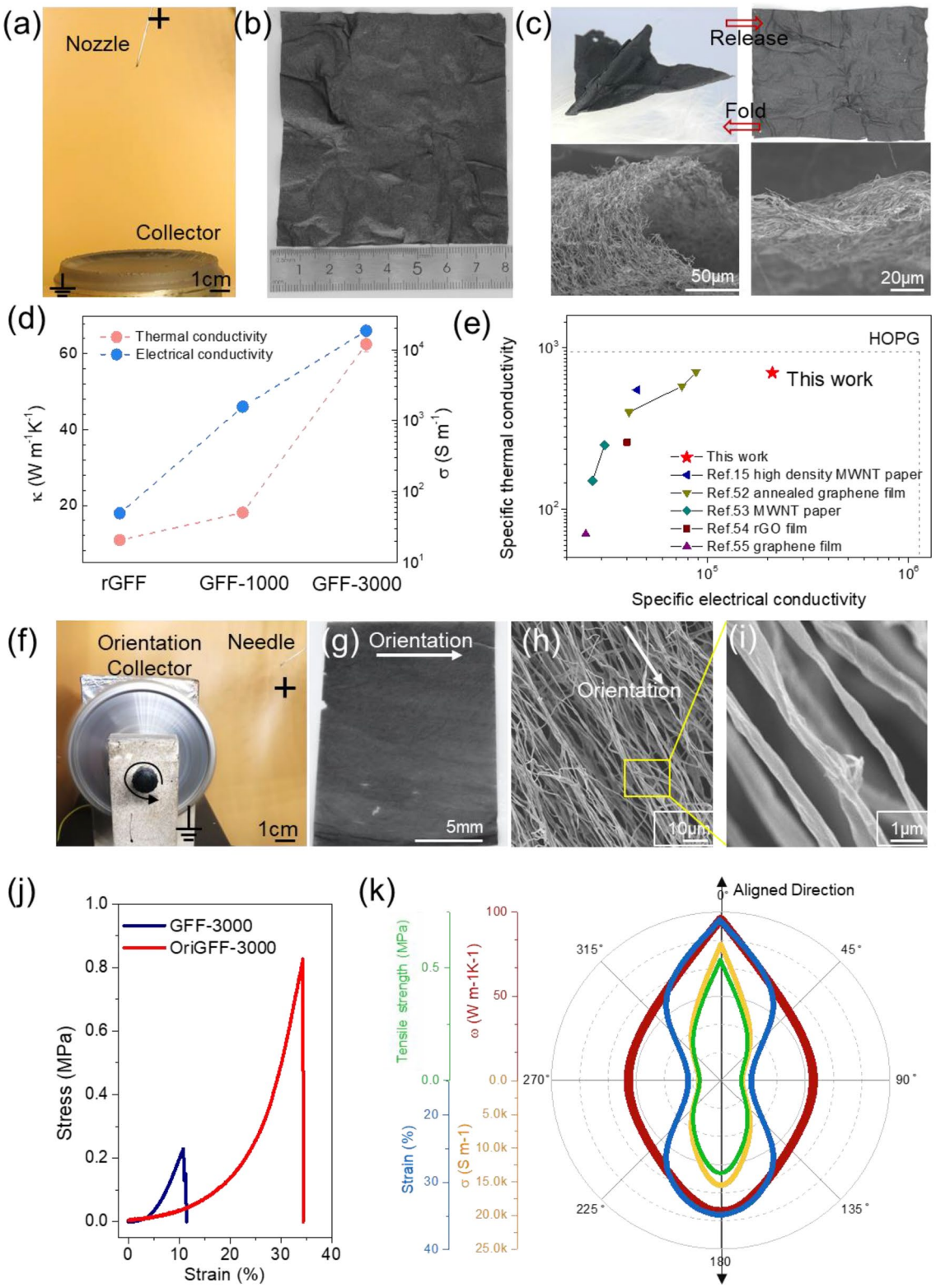
(a)
Nozzle
Collector
1cm
(b)
(c)
Release
Fold
50μm
20μm
(d)
Thermal conductivity
Electrical conductivity
κ (W m-1K-1)
σ (S m-1)
rGFF
GFF-1000
GFF-3000
(e)
HOPG
This work
Specific thermal conductivity
Specific electrical conductivity
This work
Ref.15 high density MWNT paper
Ref.52 annealed graphene film
Ref.53 MWNT paper
Ref.54 rGO film
Ref.55 graphene film
(f)
Orientation
Collector
Needle
1cm
(g)
Orientation
5mm
(h)
Orientation
10μm
(i)
1μm
(j)
GFF-3000
OriGFF-3000
Stress (MPa)
Strain (%)
(k)
Aligned Direction
Tensile strength (MPa)
ω (W m-1K-1)
Strain (%)
σ (S m-1)

◂**Fig. 4** GNF fabrics. **a** and **b** Photographs of the non-orientation collecting and the collected large-area fabric with randomly aligned texture. **c** Photographs and SEM images of the non-woven fabrics under folded and released states, showing good flexibility. **d** In-plane electrical and thermal conductivities of GFFs. **e** The comparison of specific electrical conductivity (σ/ρ) and specific thermal conductivity (κ/ρ) of GFF-3000 with previous carbon fabrics and films. **f** and **g** Photos of the rotating drum collecting and the collected fabric with well-aligned texture. **h** and **i** SEM images of the oriented texture of GNFs. **j** Typical stress–strain curves of GFF-3000 and oriented GFFs (OriGFF-3000). **k** Properties of OriGFF-3000 measured at different angles. The units for σ, ρ and κ are S m^{-1}, g cm^{-3} and W m^{-1} K^{-1}, respectively

Supplementary Information The online version contains supplementary material available at https://doi.org/10.1007/s42765-021-00105-8.

Acknowledgements Z.P.H, J.Q.W and S.P.L contributed equally to this work. The authors thank the members of staff at SSRF for SAXS characterizations. This work is supported by the National Natural Science Foundation of China (Nos. 52090030, 51973191, 51533008, 51803177 and 51873191), Hundred Talents Program of Zhejiang University (188020*194231701/113), National Key R&D Program of China (No. 2016YFA0200200), Key research and development plan of Zhejiang Province (2018C01049), Fujian Provincial Science and Technology Major Projects (NO. 2018HZ0001-2), the Fundamental Research Funds for the Central Universities (NO. K20200060), Key Laboratory of Novel Adsorption and Separation Materials and Application Technology of Zhejiang Province (512301-I21502), Shandong Provincial Natural Science Foundation (ZR2019YQ19), Project of Shandong Province Higher Educational Science and Technology Program (2019KJA026) and State Key Laboratory for Modification of Chemical Fibers and Polymer Materials, Donghua University(KF2110).

Declaration

Conflict of interest There is no conflict of interest in the article.

References

1. Chen L-F, Lu Y, Yu L, Lou XW. Designed formation of hollow particle-based nitrogen-doped carbon nanofibers for high-performance supercapacitors. *Energy Environ Sci*. **2017**;*10*:1777.
2. Malekpour S, Balkus K, Ferraris J. Hybrid supercapacitors using electrodes from fibers comprising polymer blend-metal oxide composites with polymethacrylic acid as chelating agent. *Nanotechnology*. **2021**;*32*:325401.
3. Razavi S, Neisiany R, Razavi M, Das O. Efficient improvement in fracture toughness of laminated composite by interleaving functionalized nanofibers. *Polymer* . **2021**;*13*:2509.
4. Johansen M, Schlueter C, Tam P, Asp L, Liu F. Mapping nitrogen heteroatoms in carbon fibres using atom probe tomography and photoelectron spectroscopy. *Carbon*. **2021**;*179*:20–7.
5. Meek N, Penumadu D. Nonlinear elastic response of pan based carbon fiber to tensile loading and relations to microstructure. *Carbon*. **2021**;*178*:133–43.
6. Al Faruque M, Remadevi R, Guirguis A, Kiziltas A, Mielewski D, Naebe M. Graphene oxide incorporated waste wool/PAN hybrid fibres. *Sci Rep*. **2021**;*11*:12068.
7. Xu Z, Gao C. Graphene in macroscopic order: liquid crystals and wet-spun fibers. *Acc Chem Res*. **2014**;*47*:1267.
8. Liu Y, Liang H, Xu Z, Xi J, Chen G, Gao W, Xue M, Gao C. Superconducting continuous graphene fibers via calcium intercalation. *ACS Nano*. **2017**;*11*:4301.
9. Xu Z, Gao C. Graphene fiber: a new trend in carbon fibers. *Mater Today*. **2015**;*18*:480.
10. Li Z, Liu Z, Sun H, Gao C. Superstructured assembly of nanocarbons: fullerenes, nanotubes, and graphene. *Chem Rev*. **2015**;*115*:7046.
11. Li P, Liu Y, Shi S, Xu Z, Ma W, Wang Z, Liu S, Gao C. Highly crystalline graphene fibers with superior strength and conductivities by plasticization spinning. *Adv Funct Mater*. **2020**;*30*:2006584.
12. Xu Z, Gao C. Graphene chiral liquid crystals and macroscopic assembled fibres. *Nat Commun*. **2011**;*2*:571.
13. Xu Z, Liu Y, Zhao X, Peng L, Sun H, Xu Y, Ren X, Jin C, Xu P, Wang M, Gao C. Ultrastiff and strong graphene fibers via full-scale synergetic defect engineering. *Adv Mater*. **2016**;*28*:6449.
14. Xu Z, Sun H, Zhao X, Gao C. Ultra-strong fibers assembled from giant graphene oxide sheets. *Adv Mater*. **2013**;*25*:188.
15. Zhang L, Zhang G, Liu C, Fan S. High-density carbon nanotube buckypapers with superior transport and mechanical properties. *Nano Lett*. **2012**;*12*:4848.
16. Meng F, Lu W, Li Q, Byun J-H, Oh Y, Chou T-W. Graphene-based fibers: a review. *Adv Mater*. **2015**;*27*:5113.
17. Tian Q, Xu Z, Liu Y, Fang B, Peng L, Xi J, Lia Z, Gao C. Dry spinning approach to continuous graphene fibers with high toughness. *Nanoscale*. **2017**;*9*:12335.
18. Li Z, Xu Z, Liu Y, Wang R, Gao C. Multifunctional non-woven fabrics of interfused graphene fibres. *Nat Commun*. **2016**;*7*:13684.
19. Kim JH, Chang WS, Kim D, Yang JR, Han JT, Lee G-W, Kim JT, Seol SK. 3D Printing of reduced graphene oxide nanowires. *Adv Mater*. **2015**;*27*:157.
20. Singh WI, Sinha S, Devi NA, Nongthombam S, Laha S, Swain BP. Investigation of chemical bonding and electronic network of rGO/PANI/PVA electrospun nanofiber. *Polym Bull*. **2020**. https://doi.org/10.1007/s00289-020-03442-7.
21. Bao Q, Zhang H, Yang J. Graphene-polymer nanofiber membrane for ultrafast photonics. *Adv Funct Mater*. **2010**;*20*:782.
22. Mustafa MH, Zdunek A. Supercapacitor nanofiber electrodes graphene-based. *Int J Electrochem Sci*. **2017**;*12*:2917.
23. Nobuaki K, Hiroyuki N, Masaru M, Yuki Y, Rintaro O, Ali MD, Daniel PMA, Masaru T, Keiji N, Kazuharu A. Multicomponent nature underlies the extraordinary mechanical properties of spider dragline silk. *PANS*. **2021**;*31*:118.
24. Tan Y, Song Y, Zheng Q. Hydrogen bonding-driven rheological modulation of chemically reduced graphene oxide/poly (vinyl alcohol) suspensions and its application in electrospinning. *Nanoscale*. **2012**;*4*:6997–7005.
25. Li H, Zhang Z, Song N, Kwok R, Lam J, Wang L, Wang D, Tang B. Reverse thinking of the aggregation-induced emission principle: amplifying molecular motions to boost photothermal efficiency of nanofibers. *Angew Chem*. **2020**;*59*:20371–5.
26. Liang J, Huang Y, Zhang L, Wang Y, Ma Y, Guo T, Chen Y. Molecular-level dispersion of graphene into poly(vinyl alcohol) and effective reinforcement of their nanocomposites. *Adv Funct Mater*. **2009**;*19*:2297.
27. Reynolds WN, Sharp JV. Crystal shear limit to carbon fibre strength. *Carbon*. **1974**;*12*:103.
28. Zhao X, Zheng B, Huang T, Gao C. Graphene-based single fiber supercapacitor with a coaxial structure. *Nanoscale*. **2015**;*7*:9399.
29. Zheng B, Huang T, Kou L, Zhao X, Gopalsamy K, Gao C. Graphene fiber-based asymmetric micro-supercapacitors. *J Mater Chem A*. **2014**;*2*:9736.

30. Bhardwaj N, Kundu SC. Electrospinning: a fascinating fiber fabrication technique. *Biotechnol Adv*. **2010**;*28*:325.
31. Huang ZM, Zhang YZ, Kotaki M, Ramakrishna S. A review on polymer nanofibers by electrospinning and their applications in nanocomposites. *Compos Sci Technol*. **2003**;*63*:2223.
32. Xin G, Yao T, Sun H, Scott SM, Shao D, Wang G, Lian J. Highly thermally conductive and mechanically strong graphene fibers. *Science*. **2015**;*349*:1083.
33. Jayaprakash GK, Flores-Moreno R. Quantum chemical study of Triton X-100 modified graphene surface. *Electrochim Acta*. **2017**;*248*:225.
34. Jang W, Yun J, Park Y, Park IK, Byun H, Lee CH. Polyacrylonitrile nanofiber membrane modified with Ag/GO composite for water purification system. *Polymer*. **2020**;*12*:2441.
35. Li H, Song Z, Zhang X, Huang Y, Li S, Mao Y, Ploehn HJ, Bao Y, Yu M. Ultrathin, molecular-sieving graphene oxide membranes for selective hydrogen separation. *Science*. **2013**;*342*:95.
36. Wilke S, Guyon E, Demarsily G. Water penetration through fractured rocks test of a tridimensional percolation description. *Math Geol*. **1985**;*17*:17.
37. Xue J, Wu T, Dai Y, Xia Y. Electrospinning and electrospun nanofibers: methods, materials, and applications. *Chem Rev*. **2019**;*119*:5298.
38. Chang W-M, Wang C-C, Chen C-Y. The combination of electrospinning and forcespinning: effects on a viscoelastic jet and a single nanofiber. *Chem Eng J*. **2014**;*244*:540.
39. Zong XH, Kim K, Fang DF, Ran SF, Hsiao BS, Chu B. Structure and process relationship of electrospun bioabsorbable nanofiber membranes. *Polymer*. **2002**;*43*:4403.
40. Teo WE, Ramakrishna S. A review on electrospinning design and nanofibre assemblies. *Nanotechnology*. **2006**;*17*:R89.
41. Reneker DH, Yarin AL. Electrospinning jets and polymer nanofibers. *Polymer*. **2008**;*49*:2387.
42. Wang C, Lan L, Tan H. The physics of wrinkling in graphene membranes under local tension. *Phys Chem Chem Phys*. **2013**;*15*:2764.
43. Chang IL, Chen J-A. The molecular mechanics study on mechanical properties of graphene and graphite. *Appl Phys A Mater*. **2015**;*119*:265.
44. Behabtu N, Young CC, Tsentalovich DE, Kleinerman O, Wang X, Ma AWK, Bengio EA, ter Waarbeek RF, de Jong JJ, Hoogerwerf RE, Fairchild SB, Ferguson JB, Maruyama B, Kono J, Talmon Y, Cohen Y, Otto MJ, Pasquali M. Strong, light, multifunctional fibers of carbon nanotubes with ultrahigh conductivity. *Science*. **2013**;*339*:182.
45. Cancado LG, Takai K, Enoki T, Endo M, Kim YA, Mizusaki H, Jorio A, Coelho LN, Magalhaes-Paniago R, Pimenta MA. General equation for the determination of the crystallite size L-a of nanographite by Raman spectroscopy. *Appl Phys Lett*. **2006**;*88*:163106.
46. Kudin KN, Ozbas B, Schniepp HC, Prud'homme RK, Aksay IA, Car R. Raman spectra of graphite oxide and functionalized graphene sheets. *Nano Lett*. **2008**;*8*:36.
47. Jung DK, Roh J-S, Kim M-S. Effect of carbonization temperature on crystalline structure and properties of isotropic pitch-based carbon fiber .*Carbon Lett*. **2017**;*21*:51.
48. Whiteway E, Yang W, Yu V, Hilke M. Time evolution of the growth of single graphene crystals and high resolution isotope labeling. *Carbon*. **2017**;*111*:173.
49. Wang Q, Li Y, Jin S, Sang S. Catalyst-free hybridization of silicon carbide whiskers and expanded graphite by vapor deposition method. *Ceram Int*. **2015**;*41*:14359.
50. Chen J, Kong Q, Liu Z, Bi Z, Jia H, Song G, Xie L, Zhang S, Chen C-M. High yield silicon carbide whiskers from rice husk ash and graphene: growth method and thermodynamics. *ACS Sustain Chem Eng*.**2019**;*7*:19027.
51. Li T-T, Wang Y, Peng H-K, Zhang X, Shiu B-C, Lin J-H, Lou C-W. Lightweight, flexible and superhydrophobic composite nanofiber films inspired by nacre for highly electromagnetic interference shielding. *Compos Part A Appl Sci Manuf*. **2020**;*128*:105685.
52. Xin G, Sun H, Hu T, Fard HR, Sun X, Koratkar N, Borca-Tasciuc T, Lian J. Large-area freestanding graphene paper for superior thermal management. *Adv Mater*. **2014**;*26*:4521.
53. Wang D, Song P, Liu C, Wu W, Fan S. Highly oriented carbon nanotube papers made of aligned carbon nanotubes. *Nanotechnology*. **2008**;*19*:075609.
54. Zhang M, Wang Y, Huang L, Xu Z, Li C, Shi G. 3D printing of reduced graphene oxide nanowires. *Adv Mater*. **2015**;*27*:6708.
55. Liang Q, Yao X, Wang W, Liu Y, Wong CP. A three-dimensional vertically aligned functionalized multilayer graphene architecture: an approach for graphene-based thermal interfacial materials. *ACS Nano*. **2011**;*5*:2392.
56. Kumar S, Anderson DP, Crasto AS. AFM, SEM AND XPS characterization of pan-based carbon-fibers etched in oxygen plasmas. *J Mater Sci*. **1993**;*28*:423.
57. von Sturm F. Graphite fibers and filaments. *Adv Mater*. **1989**;*1*:130.
58. Shi W, Hu B, Zhang H, Li J, Yang J, Liu J. Carbon-encapsulated iron oxide nanoparticles in self-supporting carbon nanofiber for high-performance supercapacitor in acid electrolyte with superior stability. *ACS Appl Energ Mater*. **2020**;*3*:12652–61.
59. Xie F, Wang Y, Zhou L, Jia F, Ning D, Lu Z. Electrospun wrinkled porous polyimide nanofiber-based filter via thermally induced phase separation for efficient high-temperature PMs capture. *ACS Appl Mater Inter*. **2020**;*12*:56499–508.
60. Yang Y, Xu Y, Liu Z, Huang H, Fan X, Wang Y, Song Y, Song C. Novel solvent-resistant nanofiltration membranes using MPD co-crosslinked polyimide for efficient desalination. *J Membr Sci*. **2020**;*616*:118563.
61. Amiri A, Conlee B, Tallerine I, Kennedy W, Naraghi M. A novel path towards synthesis of nitrogen-rich porous carbon nanofibers for high performance supercapacitors. *Chem Eng J*. **2020**;*399*:788.
62. Xiang S, Zhang N, Fan X. From fiber to fabric: progress towards photovoltaic energy textile. *AFMs*. **2020**;*3*:76–106.
63. AlMamun M, Islam M, Islam M, Sowrov K, Hossain M, Ahmed D, Shahariar H. Scalable process to develop durable conductive cotton fabric. *AFMs*. **2020**;*2*:291–301.
64. Wang W, Yu A, Zhai J, Wang Z. Recent progress of functional fiber and textile triboelectric nanogenerators: towards electricity power generation and intelligent sensing. *AFMs*. **2021**. https://doi.org/10.1007/s42765-021-00077-9.

Zhanpo Han is a Master student of Material Science and Engineering from Qingdao University. His research interests mainly focus on the macroscopically assembled materials of 2D materials, and high-performance materials of biological macromolecules.

Jiaqing Wang received his Ph.D. degree from University of Science and Technology of China in 2015. He is currently a postdoctoral researcher at the Department of Polymer Science and Engineering of Zhejiang University. His research interests mainly focus on the macroscopically assembled materials from 2D materials, scaling law and 2D macromolecular behavior in nanoscale.

Yeqiang Tan is a professor in College of Materials Science and Engineering, Qingdao University, China. He received his doctorate from Zhejiang University in China in 2013. He is mainly engaged in the research of polymer processing rheology and high performance fibers.

Senping Liu is a Ph.D. student in Zhejiang University. He is working on the dynamics of 2-dimensional macromolecule and fabrication of composites of polymer and graphene.

Shiyu Luo received her bachelor degree of Engeineering in Polymer Materials andEngineering at Sichuan University and has been a Ph.D student in Zhejiang University of Polymer Science and Engineering under the supervision of Prof. Chao Gao since 2019. She is working on the graphene nanofilm now.

Qinghua Zhang is a professor of Donghua University. His research includes polyimide material, high-performance fibers and organic/inorganic nanocomposites, etc.

Fan Guo received her Ph.D. degree in chemistry in Zhejiang University in 2020. She did postdoctoral research at Zhejiang University after graduation. Her research interests cover graphene macroscopic materials, and lightweight materials.

Yingjun Liu received his Ph.D. degree from Zhejiang University in 2017. He joined the Department of Polymer Science and Engineering, Zhejiang University in 2020. His research interests mainly focus on the macroscopic assembly and application of graphene-based materials, such as high performance and multifunctional graphene films and fibers.

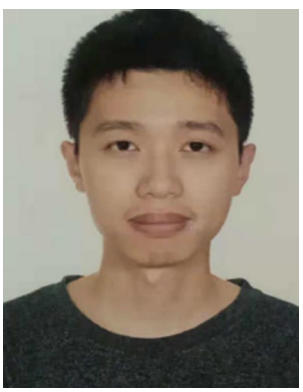

Jingyu Ma received his B.S. degrees from Zhejiang University in 2019. He is currently pursuing his Ph.D. degree under the supervision of Prof. Zhen Xu at Zhejiang University, China. His research focuses on the 2D colloidal liquid crystals and functional nanofibers.

Peng Li received his Ph. D. degree in Chemistry in Zhejiang University in 2021. Then he continued his postdoctoral research in Prof. Chao Gao`s lab at Zhejiang University. His research interests involve structural-functional integrating carbonaceous fibers, graphene macroscopic materials with combination of high strength and high toughness, and bio-inspired graphene frameworks.

Xin Ming is currently a Ph.D. student at Department of Polymer Science and Engineering of Zhejiang University under the supervision of Prof. Chao Gao. His current research interests are graphene-based materials and assembly for multifunctional applications, especially for high-performance fiber materials.

Chao Gao is a"Qiushi Distinguished Professor"of Zhejiang University. He receivedhis Ph.D. at Shanghai Jiao Tong University in 2001. His research interests include graphene chemistry and graphene macroscopic self-assembly.

Zhen Xu received his Ph.D. degree in chemistry in Zhejiang University in 2013. He did postdoctoral research at Zhejiang University in 2013–2015 and at Cambridge Graphene Center at Cambridge University from 2015 to 2016. In 2017, he joined the Department of Polymer Science and Engineering, Zhejiang University, as a Research Professor. His research interests cover liquid crystals of 2D nanomaterials, graphene macroscopic materials, and 2D macromolecular behavior.